Biomedicine & Pharmacotherapy 139 (2021) 111587

Contents lists available at ScienceDirect

Biomedicine & Pharmacotherapy

journal homepage: www.elsevier.com/locate/biopha

Original article

Salvia-Nelumbinis naturalis extract protects mice against MCD diet-induced steatohepatitis via activation of colonic FXR-FGF15 pathway

Chunlin Li [a,1], Wenjun Zhou [a,1], Meng Li [a], Xiangbing Shu [b], Li Zhang [a,*], Guang Ji [a,*]

[a] Institute of Digestive Diseases, Longhua Hospital, Shanghai University of Traditional Chinese Medicine, Shanghai 200032, China
[b] Department of Geratology, Baoshan Branch of Shuguang Hospital, Shanghai University of Traditional Chinese Medicine, Shanghai 201999, China

ARTICLE INFO

Keywords:
Salvia-Nelumbinis naturalis
Steatohepatitis
Gut microbiota
NorDeoxycholic acid
Farnesoid X receptor
Fibroblast growth factor 15

ABSTRACT

Salvia-Nelumbinis naturalis (SNN) formula is a traditional Chinese medicine prescription, and has been confirmed to be effective in treating non-alcoholic steatohepatitis (NASH), but the underlying mechanisms are still unknown. Here we showed that 4-week SNN administration alleviated methionine-choline-deficiency (MCD) diet-induced hepatic steatosis and inflammation as well as serum levels of alanine transaminase (ALT) increase in C57BL/6 mice. Fecal 16S rDNA sequencing indicated that SNN altered the structure of gut microbiota and partially reversed the gut dysbiosis. Simultaneously, we analyzed the fecal BA profile using liquid chromatography coupled with triple quadrupole mass spectrometry (UPLC-TQMS) -based metabolomics, and found that SNN modulated fecal BA profile, predominantly increased the microbiomes related BA species (e.g. nordeoxycholic acid) which in turn, activated farnesoid X receptor (FXR)-fibroblast growth factor 15 (FGF15) signaling pathway in the colon but not the ileum. The activation of intestinal FXR-FGF15 signaling was accompanied by increase of liver protein kinase B (PKB/Akt) phosphorylation, and decrease of p-65 subunit of NF-κB phosphorylation, resulting in less liver CD68 positive macrophages, and inflammatory cytokine IL-1β and TNF-α expression. Our results established the link between SNN treatment, gut microbiota, BA profile and NASH, which might shed light into the mechanisms behind the beneficial effects of SNN on NASH, thus provide evidence for the clinical application of SNN.

1. Introduction

Nonalcoholic steatohepatitis (NASH) is the progressive form of nonalcoholic fatty liver disease (NAFLD), characterized by liver steatosis and infiltration of inflammatory cells, which potentiates a risk for progressive fibrosis, cirrhosis, and end-stage liver disease [1,2]. As the increased incidence of NAFLD, the aggravated NASH has become the second leading cause of liver transplantation in the US [2], and the number of NASH patients on the waiting list is still rising [3]. In addition, NASH is associated with increased incidence of type 2 diabetes, atherosclerosis, and coronary heart disease [4].

Dysfunction of gut microbiota contributes to the NASH development and progression. Recent studies suggest that metabolites of gut microbiomes, such as short-chain fatty acids [5,6], branched-chain amino acids [7,8] and bile acids (BAs) [9,10], may have unique therapeutic promise for NASH. Among these metabolites, BAs are of specific concern. BAs are synthesized in the liver, secreted into intestine, and can be recycled 4–12 times per day in the distal ileum. The continuous enterohepatic circulation of BAs provides facility for the mutual modulation with gut microbiomes. The functions of BAs are conducted mainly through BA receptors such as farnesoid X receptor (FXR) and G protein coupled bile acid receptor-1 (TGR5) [11]. In the colon, hepatocyte synthesized primary BAs can be converted into secondary BAs by the action of certain microbiomes, and re-enter the BA enterohepatic circulation [12,13]. Activation of intestinal FXR induces fibroblast growth factor (FGF15 in rodents, and FGF19 in human) secretion, which enters the liver to exert pleiotropic functions through binding fibroblast growth factor receptor 4 (FGFR4) [13].

Currently, no approved pharmacologic therapy is available whereas the management of NASH is in urgent need. Traditional Chinese medicine is one of important choices for treating NASH. Classic or designed formulae that comprised multiple herbs are widely used in Asia countries. The designed formula Salvia-Nelumbinis naturalis (SNN) has been founded to be effective in treating NAFLD [14,15]. Herbal products

* Corresponding authors.
E-mail addresses: zhangli.hl@163.com (L. Zhang), jiliver@vip.sina.com (G. Ji).
[1] Equally contribute.

https://doi.org/10.1016/j.biopha.2021.111587
Received 9 December 2020; Received in revised form 31 March 2021; Accepted 2 April 2021
Available online 14 April 2021

usually serve as substrates for gut microbiota, and we have revealed that SNN treatment remodeled gut microbiota, increased the relative abundance of *Ruminococcaceae* and *Lachnospiraceae*, and decreased the relative abundance of *Desulfovibrionales* and *Campylobacterales* in high-fat-dextran sulfate sodium-induced NASH mice [16]. Since microbiomes are in close relation to BA conversion and metabolism [11,12,17], the gut microbiota-BA interaction arises great concern in studying BA homeostasis, lipid metabolism as well as metabolic inflammation.

In the present study, we showed that SNN potently improved hepatic lipid accumulation and inflammation in mice fed a methionine-choline-deficiency (MCD) diet. We further found that SNN treatment remodeled MCD diet-induced gut dysbiosis and fecal BA profile by applying 16S ribosomal DNA (rDNA)-based microbiota analysis and liquid chromatography coupled with triple quadrupole mass spectrometry (UPLC-TQMS)-based fecal BA metabolomics. The alteration of BA profile upon SNN treatment, e.g. norDCA increase, might contribute to the activation of colonic FXR-FGF15 signaling pathway, which improves hepatic insulin resistance and inflammation. The results of this study demonstrated a mechanistic link between SNN, alteration in the gut microbiomes and BA profile, and intestinal FXR signaling in the modulation of MCD diet-induced NASH.

2. Materials and methods

2.1. Preparation of SNN extract

The SNN formula was provided by Longhua Hospital, Shanghai University of Traditional Chinese medicine. Voucher samples (No. DFREC-QC-YP-033) were stored in the cabinet of the Institute of Digestive Diseases. The extract was prepared and quality control was conducted according to the method we described in our previous studies [18,19].

2.2. Animals and diet

Male C57BL/6 mice, six weeks of age (18–20 g), were purchased from Beijing Vitalriver Experimental Animal Technology Co. LTD, and maintained in a controlled temperature (22 ± 2 °C) and humidity (55 ± 15%) with a 12 h light/12 h dark cycle specific-pathogen-free environment. The mice were divided into 3 groups after 1-week acclimatization: CON group (n = 8) received chow diet as control, NASH group (n = 8) received MCD diet (Research Diet, A02082002B), and SNN group (n = 8) received MCD diet and supplemented with SNN extract. SNN extract (750 mg/kg body weight, which is the equivalent dosage of clinical use) were administered to the mice by gavage (0.1 ml/10 g body weight) once a day for 4 weeks, CON and NASH group mice were received equal volume of normal saline. At the end of the experiment, animals were weighed and injected with 2% pentobarbital sodium (1.5 ml/kg body weight) for anesthesia. Blood was collected and serum was separated for biological analysis, liver tissues were quickly removed, weighed, snap frozen in liquid nitrogen and stored at −80 °C, feces from the ileocecal junction were collected. The animals were then sacrificed via exsanguination. All animals were received humane care according to the Chinese Animal Protection Act and National Research Council criteria, and the experiment was approved by the Animal Experiment Ethics Committee of Shanghai University of Traditional Chinese Medicine (Approval number: PZSHUTCM200710011).

2.3. Liver histochemistry

Liver portions were fixed in 4% paraformaldehyde solution and processed as previously reported [20]. Paraffin-embedded blocks were cut into 4-μm-thick sections and stained with hematoxylin & eosin (H&E) reagent. Frozen liver tissues were cut into 8-μm-thick sections and stained with oil red O solution. For immunohistochemical (IHC) analysis, we performed our established protocol [21], and used anti-CD68 (Rabbit polyclonal, 1:250, Abcam) and anti-IL-1β (Rabbit polyclonal,1:100, Bioss) primary antibodies, and incubated with biotinylated goat anti rabbit IgG (BOSTER, SA1022). NAFLD activity score (NAS) of H&E staining images were evaluated by pathologists. The scoring system comprised three histological features: steatosis (0–3), lobular inflammation (0–3), hepatocellular ballooning (0–2) as reported previously [3].

2.4. Analysis of serum and liver biochemical parameters

The levels of serum alanine aminotransferase (ALT), aspartate aminotransferase (AST) and total bile acid (TBA) were analyzed by a TBA-40FR Fully Automatic Biochemical Analyzer (TOSHIBA, Japan) with corresponding kits, according to manufacturer's protocol. To quantify the liver TG and TC contents, liver tissue homogenate in ethanol was prepared, supernatant was collected and the TG and TC content were detected with the special kits (Jiancheng Bioengineering Institute, Nanjing, China).

2.5. 16S rDNA amplicon sequencing

Caecal content samples of CON group, NASH group and SNN group were selected for microbiota 16S rDNA analysis. Microbial genome DNA was extracted using the Qiagen QIAamp DNA Stool Mini Kit (Qiagen, Dusseldorf, Germany) following the manufacturer's protocol. DNA concentration and integrity were evaluated using the NanoDrop 2000 C spectrophotometer and agarose gel electrophoresis, respectively. The V3-V4 region of the bacterial 16S ribosomal RNA was amplified by PCR. The sequencing and analysis were performed as previously reported. Weighted and unweighted unifrac principle coordinate analysis (PCoA) was performed to visualize the structural variation of microbial communities across samples, the dominant ratio of *Firmicutes* to *Bacteroidetes* (F/B ratio) was calculated.

2.6. Analysis of the BA profile

The BA concentration in fecal samples were quantified using ultra performance liquid chromatography coupled with triple quadrupole mass spectrometry (UPLC-TQMS, Waters, Milford, MA) according to a previously established protocol [22,23].

2.7. Western blot analysis

Liver tissues were homogenized in ice-cold RIPA buffer containing protease and phosphatase inhibitors, and centrifuged for 30 min at 12,000×*g*. The supernatant was collected, and protein concentration was assayed using BCA kit (CWbiotech, Shanghai, China), proteins were separated by 12.5% sodium dodecyl sulfate-polyacrylamide gel and transferred onto PVDF membranes (Millipore, USA). Subsequently, the membranes were blocked for 1 h with 5% skim milk in a buffer containing 140 mmol/L NaCl, 20 mmol/L Tris-HCl (pH 7.5), and 0.1% Tween 20 and incubated with primary antibodies overnight at 4 °C: TGR5 rabbit polyclonal antibody (72608, Abcam, USA), FXR mouse monoclonal antibody (72105S, CST, USA), FGF15 mouse monoclonal antibody (514647, Santa Cruz Biotechnology, China), SHP rabbit monoclonal antibody (3759, CST, USA), P-Akt rabbit monoclonal antibody (4058S, CST, USA), Akt rabbit monoclonal antibody (2938S, CST, USA), P-P65 rabbit monoclonal antibody (3031S, CST, USA), P65 rabbit monoclonal antibody (8242S, CST, USA), β-actin (Hua-an Bio-tech Inc., Hangzhou, China), and then incubated with horseradish peroxidase conjugated secondary antibodies for another 1 h. The bands were visualized by ECL chemiluminescence detection kit (WBKLS0500, Millipore, USA) with enhanced chemiluminescence system (Tanon 5200, Shanghai, China). The bands were quantitatively analyzed by Image J and Graphpad Prism software.

Table 1
Sequences of the primers used for RT-qPCR.

Gene	Forward primer	Reverse primer
Tnfα	ACGTGGAACTGGCAGAAGAG	GGTTGTCTTTGAGATCCATGC
Fxr	CGGCTGTCAGGATTTGTGC	GAAGCCCAGGTTGGAATAGTAAG
Shp	ATCAGACCGGCCACAACC	GCCCTTCAGGTACGCATACTC
Fgf15	GATCCACTCTTTCTCTACGGCTG	CGTTCGTTTTGGTCCTCCTC
Fgfr4	CTGTATGGGCTAATGAGGGAGTG	TCAGGCGGAGGTCAAGGTAC
Cyp7a1	TTCAAGACCGCACATAAAGCC	GAGATGCCCAGAGGATCACG
Ntcp	CCTGTCTAACCTCTTCACCCTG	CTCCGTCGTAGATTCCTTTGC
GAPDH	GTGCCGCCTGGAGAAACC	GGTGGAAGAGTGGGAGTTGC

2.8. Real-time quantitative PCR

Liver tissues were homogenized in TRIzol reagent (Invitrogen Corp, Carlsbad, CA, USA) and total RNA was isolated. RNA concentration was measured using a NanoDrop 2000C spectrophotometer (Thermo Fisher Scientific, Waltham, MA, USA), and 1 μg RNA from each liver sample was transcribed into complementary DNA by reverse transcription kit (Thermo Fisher, Massachusetts, USA). The primers for PCR were designed and synthesized (Sangon Biotech, Shanghai, China) and the sequence information was shown in Table 1. Real-time quantitative PCR (RT-qPCR) was performed using SYBR Green PCR Master Mix (Applied Biosystems, Thermo Fisher Scientific, USA) and the reaction was run in an ABI 7500 StepOne Plus System (Applied Biosystems Instruments, Thermo Fisher Scientific, USA). GAPDH served as the reference housekeeping gene, and the expression of each target gene was normalized to GAPDH expression, and relative expression of target genes to GAPDH was calculated by the $2^{-\Delta\Delta T}$ method.

2.9. Statistical analysis

Phenotype, microbiota and BA data are collected from 8 different mice. Data were shown as mean ± standard deviation (SD). Statistical analysis was performed using one-way analysis of variance (ANOVA). Independent-sample *t*-test was used to compare difference between two groups. Mann-Whitney *U* tests and Spearman correlation were performed using SPSS 18.0 software. $P < 0.05$ was considered to be statistically significant.

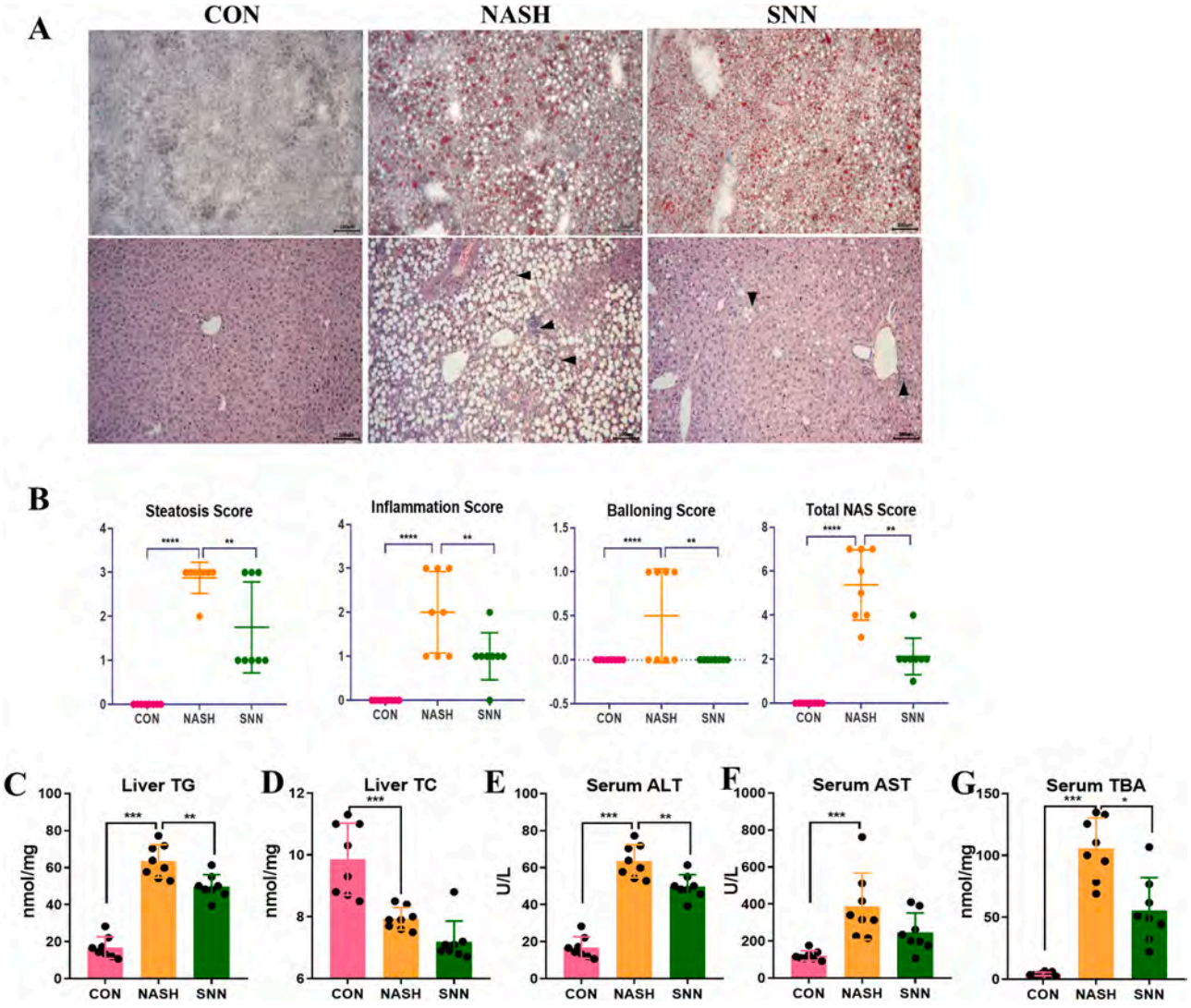

Fig. 1. SNN improved MCD diet-induced liver steatosis and inflammation. A. Representative images of Oil Red O and hematoxylin-eosin (H&E) staining of liver sections. B. The value of NAS score of the H&E stained liver sections. C and D: Liver TG and TC content. E-G: Serum ALT, AST and TBA levels. Image magnification was 200×. Data were shown as mean ± SD, n = 8 per group, *$p < 0.05$, **$p < 0.01$, ***$p < 0.001$ and ****$p < 0.0001$.

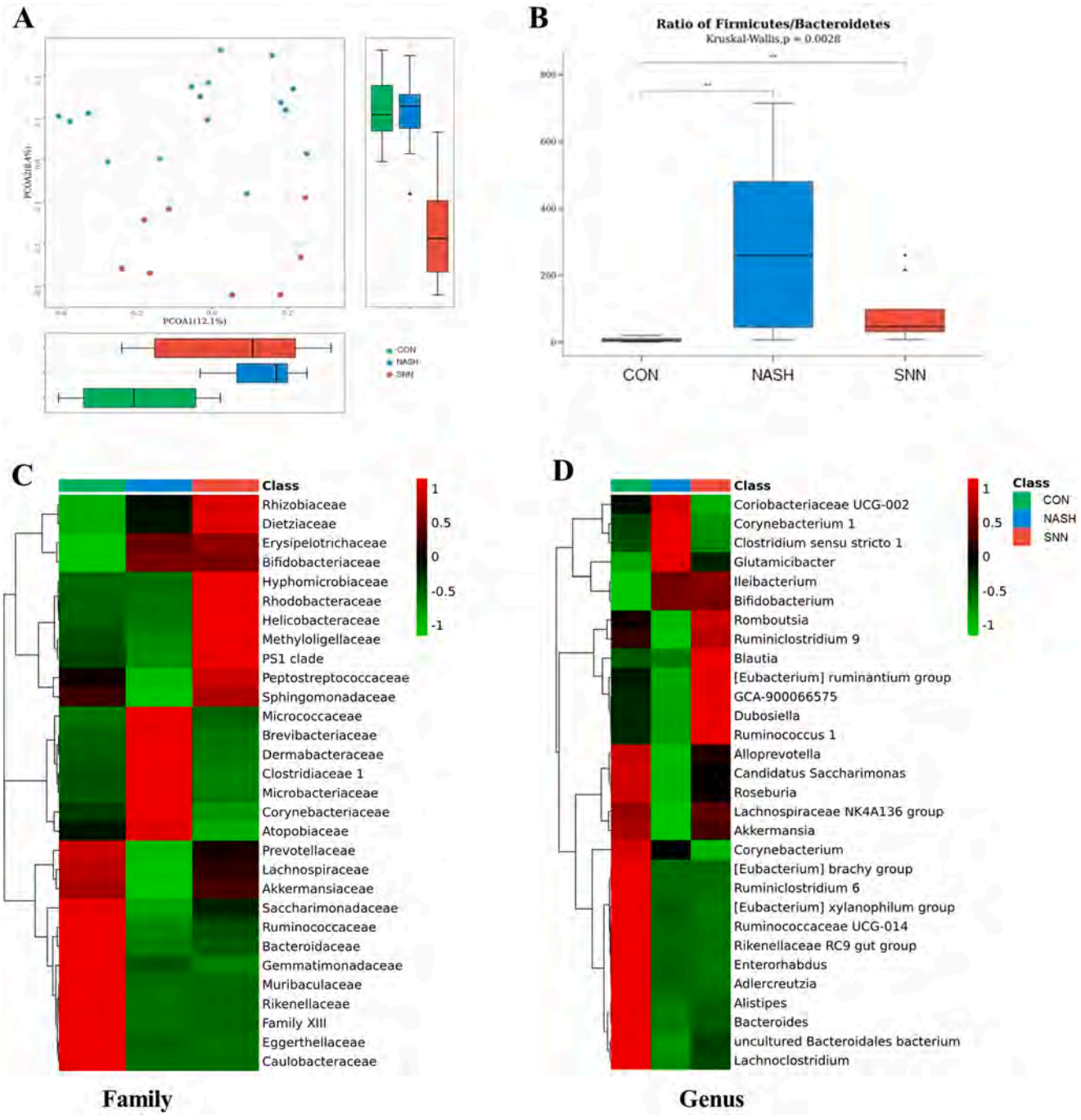

Fig. 2. SNN alleviated gut dysbiosis. A. UniFrac-based principal coordinates plot based on the OTU matrix of mouse cecum microbiota in CON, NASH, and SNN group. B. The ratio of *Firmicutes* and *Bacteroidetes*. C and D. The relative abundances of OUTs at family and genus level of CON, NASH, and SNN treatment group. n = 8 per group, $^{**}p < 0.01$.

3. Results

3.1. SNN improved MCD-diet-induced liver steatosis and inflammation

To evaluate the effect of SNN on NASH, we fed male C57BL/6 mice with MCD diet for 4 weeks, and the mice showed typical NASH features as confirmed by the presence of liver steatosis and infiltration of inflammatory cells (Fig. 1A and B), and increased TG content in the liver (Fig. 1C). SNN treatment effectively reduced liver steatosis, inflammation, ballooning and total NAS score, decreased liver TG content and serum ALT and TBA levels, but had no effect on liver TC content. These results suggested that SNN could prevent NASH development in MCD diet-fed mice.

3.2. SNN alleviated gut dysbiosis

Gut microbiota plays a critical role in the NASH development, and modulation of the microbiome is reported to be a promising strategy in treating NASH. Here we determined the structural changes of gut microbiota that in response to SNN treatment by sequencing microbial samples isolated from the cecum of the mice. PCoA revealed distinct clustering of microbiota composition for CON, NASH, and SNN treatment group (Fig. 2A). The ratio of *Firmicutes* and *Bacteroidetes* was significantly increased in NASH mice in comparison to CON mice,

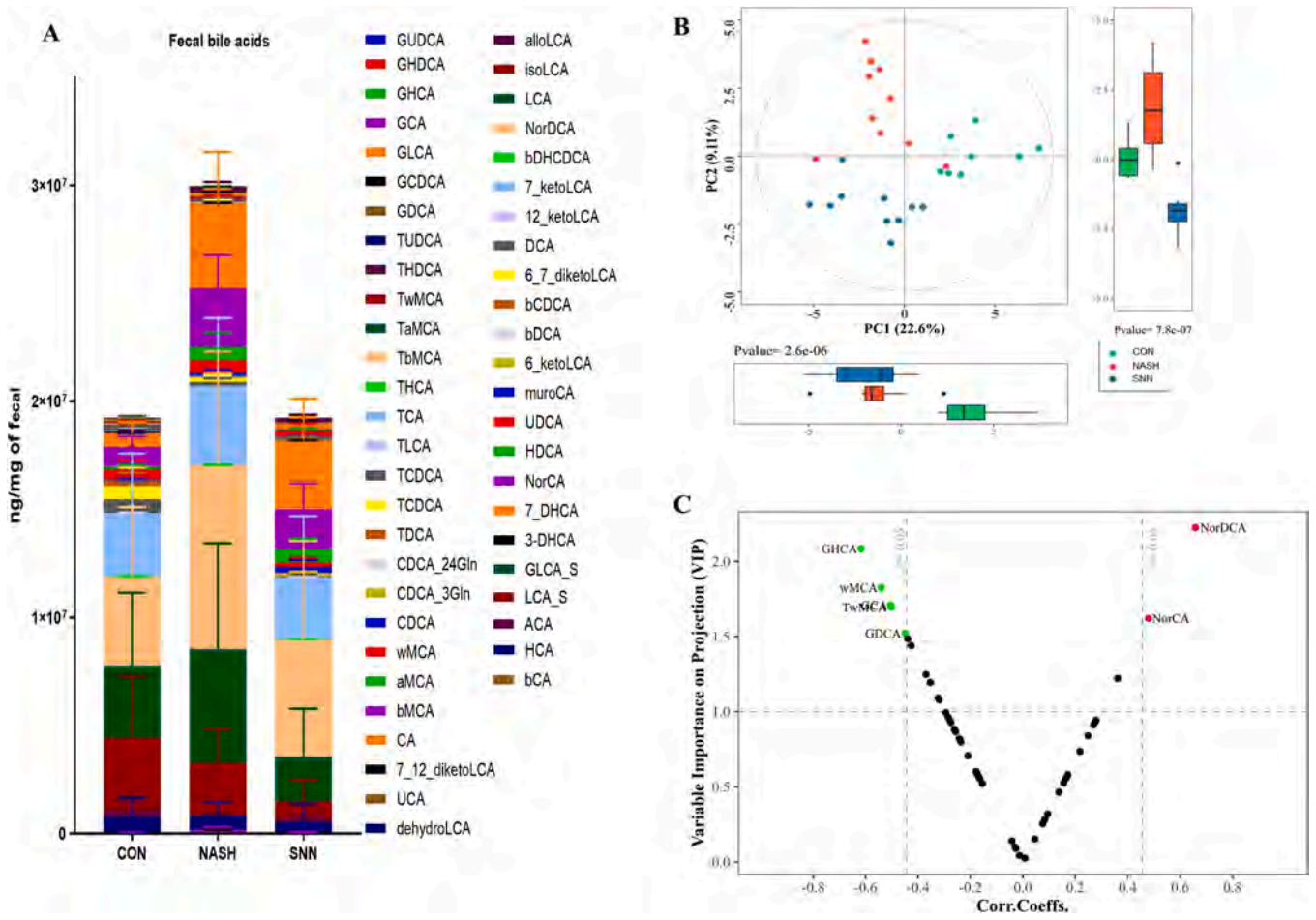

Fig. 3. SNN altered fecal BA composition. A. The composition of fecal BA in CON, NASH, and SNN treatment group. B. Partial Least Squares Discriminant Analysis (PLS-DA) of BA profile among groups. C. The variable importance in the projection model to visualize the different BAs between NASH and SNN treatment group.

whereas SNN treatment decreased the ratio (Fig. 2B).

We analyzed the degree of bacterial taxonomic similarity at the family and genus level, respectively, and assessed the change of the bacterial community that in response to SNN treatment. Family analysis revealed that SNN treatment reversed the relative abundances of OUTs in *Micrococcaceae*, *Brevibacteriaceae*, *Dermabacteraceae*, *Clostridiaceae 1*, *Microbacteriaceae*, *Corynebacteriaceae* and *Atopobiaceae* increase, and *Peptostreptococcaceae*, *Sphingomonadaceae*, *Prevotellaceae*, *Lachnospiraceae* and *Akkermansiaceae* decrease induced by MCD diet (Fig. 2C). At genus level, SNN decreased the enrichment of *Coriobacteriaceae UCG-002*, *Corynebacterium 1*, *Clostridium* sensu stricto *1and Glutamicibacter*, whereas increased *Romboutsia*, *Ruminiclostridium 9*, *Alloprevotella*, *Candidatus Saccharimonas*, *Roseburia*, *Lachnospiraceae NK4A136 group* and *Akkermansia* (Fig. 2D). These results indicated that SNN modulated the gut microbiomes, and partially reversed the gut dysbiosis of NASH mice.

3.3. SNN modulated fecal BA composition

To determine the effects of SNN on the BA profile, a UPLC/TQMS based targeted metabolomics approach was used to analyze the BAs in the feces of the mice. The results revealed that the total fecal BA levels were significantly increased in NASH mice, and SNN treatment could decrease the total BA levels (Fig. 3A). By analyzing the components of the BAs, we found that the secondary BAs were decreased in NASH mice, most significantly, TDCA, THDCA, GHDCA, and TωMCA, whereas primary BAs, such as CDCA, CA, GCA, GHCA, and norCA were remarkably increased in NASH mice (Fig. 3A). We next applied Partial Least Squares Discriminant Analysis (PLS-DA) to visualize the distinct difference among the three groups, indicating that SNN could modulate the fecal BA profile (Fig. 3B). We applied variable importance in the projection model to identify the most significant metabolites between NASH group and SNN group, and found that SNN increased fecal norDCA and norCA, and decreased GHCA, ωMCA, TωMCA, GCA and GDCA level (Fig. 3C), suggesting that CAs and DCAs might be the important BA species that in response to SNN treatment.

3.4. The correlation of SNN responded microbiomes and BAs

To indicate the relative importance of altered metabolites and microbiomes between SNN and NASH groups, we applied supervised multivariate analysis and constructed RF model, 8 microbiome species and 1 metabolite were confirmed (Fig. 4A). To visualize the correlation, a Spearman correlation was performed between the relative abundance of differential microbial species and the BAs in the SNN and NASH groups (Fig. 4B). The norDCA was negatively correlated with *Adlercreutzia* in *Actinobacteria,* and *Negativibacillus*, *Lactobacillus* and *Ruminiclostridium 6* in *Firmicutes* phyla, whereas norCA was negatively correlated with *Enteractinococus* in *Actinobacteria* and *Negativibacillus* in *Firmicutes* phyla. The TDCA and THDCA were positively correlated with *Lachnoclostridium* and *Dubosiella* in *Firmicutes* phyla and *Candidatus Saccharimmonas* in *Patescibacteria* phyla. A network plot was drawn to show the positive and negative correlations between microbiomes and BAs (Fig. 4**C**).

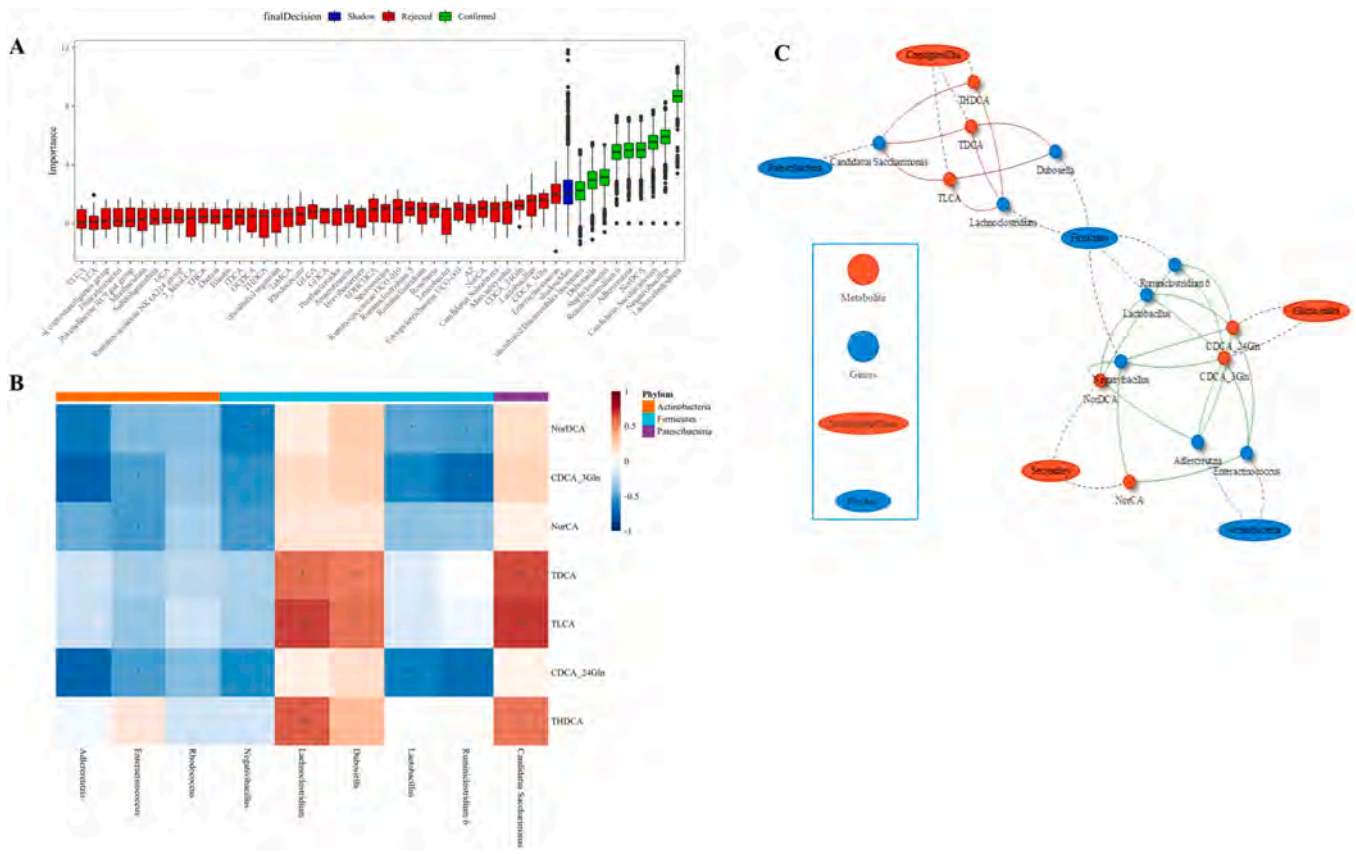

Fig. 4. The correlation of SNN responded microbiomes and BAs. A. Supervised multivariate analysis and RF model. B. Spearman correlation analysis of the relative abundance of microbial species and the BAs. C. A network plot of correlations of microbiomes and BAs.

3.5. SNN activated colonic FXR-FGF15 pathway

The alteration of intestinal BA profile may affect BA receptors, we next detected the expression of typical BA receptors, TGR5 and FXR, in both the ileum and colon of the mice. The relative protein expression of TGR5 was not statistically different among groups in both colon and ileum (Fig. 5A and B). The nuclear BA receptor FXR was significantly decreased in colon and ileum of NASH mice, and SNN intervention only increased the colonic FXR expression (Fig. 5A and B). Intestinal FXR activation would promote FGF15 secretion, and we found that SNN intervention reversed the relative protein expression of colonic FGF15 in NASH mice accordingly (Fig. 5A). We also detected liver FXR and SHP, although the relative protein expression was decreased in NASH mice, SNN did not show any effect on liver FXR expression (Fig. 5C). The SHP expression in the liver did not show statistical difference among groups either (Fig. 5C). We also analyzed other BA metabolism related molecules in the liver, and found that SNN reversed the FGF15 mRNA expression, but has no effect on FXR or BA synthesis or transportation related molecules in liver (Fig. 5D). These results suggested that colonic FXR-FGF15 pathway activation may contribute to the beneficial effects of SNN on NASH mice.

3.6. SNN suppressed liver metabolic inflammation

Intestinal FXR-FGF15 signaling plays a role in regulating hepatic inflammatory and insulin pathway. We analyzed the liver extracts, and found that SNN treatment increased the ratio of phosphorylated AKT to total AKT and decreased the ratio of phosphorylated p65 to total p65 (Fig. 6A), indicating enhanced hepatic insulin sensitivity and reduced inflammatory status upon SNN treatment. We further assessed the impact of SNN on macrophages and inflammatory cytokines. Compared with the NASH mice, the SNN-treated mice showed decreased CD68 positive area (Fig. 6B), indicating less macrophage accumulation in the liver upon SNN treatment. Accordingly, the liver IL-1β expression was also decreased in SNN treatment mice (Fig. 6B). In addition, SNN administration also reduced *Tnfα* mRNA expression in hepatic tissues (Fig. 6C). These results implied that SNN exhibits robust efficacy against metabolic and immune disorders in NASH mice.

4. Discussion

NASH is becoming one of the most common and health-threatening diseases, and the global NASH market is of great potential (www.reportsanddata.com). Although over 30 clinical trials are ongoing, there is still no approved drug for NASH up to now. The widely recognized "multiple hits" hypothesis indicates that multiple insults are involved in NASH development. TCM formulae are attractive candidates for NASH due to the multiple components as well as effectiveness and safety. Here, we found that 4-week SNN treatment remarkably alleviated NASH phenotype in mice fed with MCD diet, the beneficial effects may attribute to the modulation of gut dysbiosis and microbiome related BAs, which then activated colonic FXR-FGF15 pathway (Fig. 7). Our data indicates that SNN might be a promising agent for NASH through modulating microbiomes and BAs.

Gut microbiomes actively participate in regulating host metabolism, and are mutualist partners of the host. Clinical investigations suggested imbalance or maladaptation of gut microbiota is common in NASH patients, and modification of the microbiota with antibiotics or tempol is

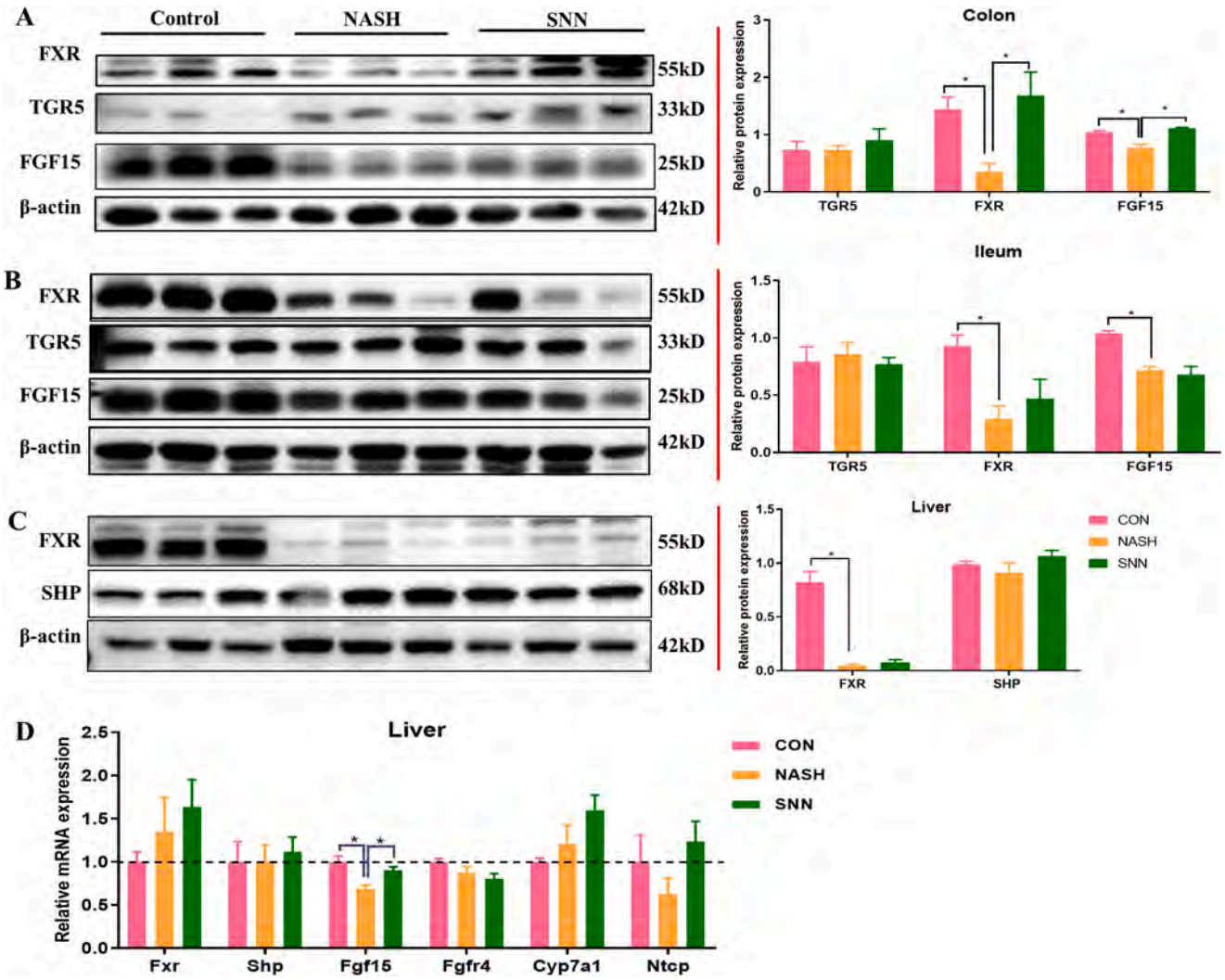

Fig. 5. SNN promoted colonic FXR-FGF15 pathway. A-C: Expression of FXR, TGR5, FGF15 and SHP in colon, ileum and liver were assayed by Western blot, n = 3 per group. D: Expression of liver *Fxr*, *Shp*, *Fgf15*, *Fgfr4*, *Cyp7a1* and *Ntcp* were detected by RT-qPCR, n = 8 per group. Data were shown as mean ± SD, $^*p < 0.05$.

found to be beneficial. The gut has the largest number of bacteria and the greatest number of species. Of the microbiota that residents in the gut, *Firmicutes* and *Bacteroidetes* are the dominating microbiomes, and the F/B ratio is reported to rise in obese and NASH patients [24,25]. Exercise or diet intervention can decrease F/B ratio, and improve gut dysbiosis and metabolic disorders [26,27]. Here we observed that SNN treatment reversed the increased F/B ratio in NASH mice, which may attribute to the modulation of gut dysbiosis. At the genus level, SNN treatment enriched the *Lactobacillus* and *Alloprevotella*, which are considered to be beneficial. It is reported that the relative abundance of *Lactobacillus* and *Alloprevotella* are decreased in mice fed with high-fat or high-sucrose diet, whereas probiotics treatment could reverse the trend [28]. The abundance of *Akkermansia* genus is reported to be increased upon the antibiotic administration [29], and we also found the increased abundance of *Akkermansia* genus upon SNN treatment.

The secondary BA formation needs multi-step 7α-dehydroxylation reaction and certain microbiomes that could produce the enzymes. Notably, *Lactobacillus* and *Ruminiclostridium* are actively involved. *Lactobacillus* is a bile salt hydrolase (BSH) producing microbiome, and *Lactobacillus* mucosae DPC 6426 is found to specifically hydrolyze the glyco-conjugated BAs [30,31]. *Ruminiclostridium* (*Clostridium*) is a 7-dehydroxylating bacteria, and catalyzes DCA/LCA formation in the gut [32]. We constructed the relationship network of SNN regulated microbiomes and BA species, and found that the altered BA species are in close association with *Actinobacteria*, *Firmicutes*. *Actinobacteria* is belong to the order *Actinomycetales*, and important source of Streptomyces, thus processes pharmacological potential [33]. *Negativibacillus* is found to be related to the immunomodulatory effect in the colon [34]. Here we established the network of confirmed BA species with microbiomes that responsive to SNN treatment, and highlighted the alteration of norDCA. NorDCA is formally named as (3α,5β,12α)-3,12-dihydroxy-24-norcholan-23-oic acid, and is a 23-carbon derivative of DCA. A recent study detected norDCA in rats, and found that the level of norDCA is decreased in NAFLD rats [35]. However, the function of norDCA is still unknown. It is reported that the nor-form of UDCA is more hydrophilic and less toxic than UDCA, norUDCA obtains the ability to stimulate bicarbonate secretion and protect cholangiocytes and hepatocytes from apolar hydrophobic BA exposure, and is considered as a better drug for primary sclerosing cholangitis and NAFLD [36,37]. Thus, we speculated that the nor form of DCA might be an active metabolite, and the exact functions need to be explored.

BAs exert their hormonal functions through binding to their receptors. FXR and TGR5 are the mostly studied BA receptors. We analyzed the both TGR5 and FXR in ileum and colon, and found the

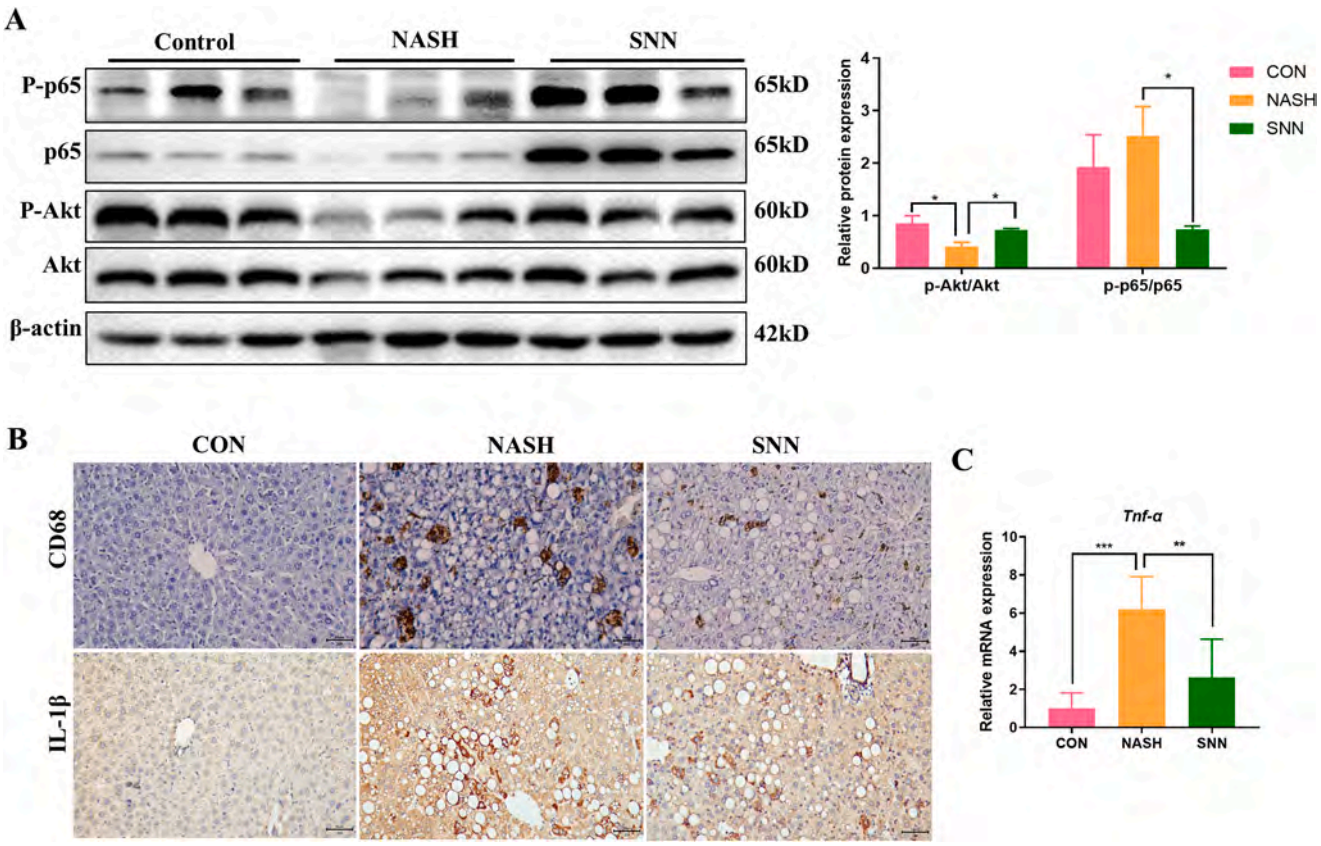

Fig. 6. SNN suppressed hepatic metabolic inflammation. A: Expression of liver P-P65, P65, P-Akt and Akt were assayed using Western blot, n = 3 per group. B: Expression of liver CD68 and IL-1β was detected by IHC staining. C: Expression of liver *Tnfα* were detected by RT-qPCR, n = 8 per group. Data were shown as mean ± SD, $*p < 0.05$, $**p < 0.01$, $***p < 0.001$.

intestinal FXR up-regulation upon SNN treatment. FXR is widely expressed in the intestine, and tightly controls the enterohepatic BA homeostasis. Activation of intestinal FXR is reported to improve metabolic disorders in *db/db* mice [38]. However, other studies showed that intestinal FXR antagonist to be beneficial in obesity mice [39,40]. Thus, intestinal FXR might exert bidirectional regulation of metabolic diseases. FXR deficiency could increase hepatic steatosis and alter BA pool composition, contributing to worsened liver toxicity induced by ethanol [41]. Intestine-restricted FXR agonist fexaramine is reported to improve metabolic disorder partly through stimulating intestinal FGF15 production [42]. In addition, activation of intestinal FXR can counter LPS-induced impaired intestinal epithelial barrier [43], which may be in association with the reduction of bacterial translocation to the liver in cirrhosis [44]. Here we revealed that SNN treatment activated intestinal FXR-FGF15 signaling pathway, and modulated hepatic disorders. Similarly, with low bioavailability, both berberine and Pu-er tea inhibited BSH activity and increased the levels of tauro-conjugated bile acids in the gut, which is associated with intestinal FXR activation, the beneficial effects are found to be lost in intestinal FXR knock out mice [45].

The microbiome-producing secondary BAs also enter the enterohepatic circle, and may affect other tissues. Here we detected FXR-SHP pathway in the liver, and found that the hepatic FXR and SHP expression have no statistical difference between NASH mice and SNN treatment mice, suggesting that the effect of SNN on liver FXR is limited. Accordingly, our previous work found the alteration of secondary BA (LCA) upon treatment in the intestine, but the secondary BA profile in the liver and serum was almost unaffected [21]. We also found the decrease of TBA upon SNN treatment, which may also be associated with the FXR expression in the liver.

In conclusion, our findings indicated that SNN could modulate gut microbiota and intestinal BA profile, the alteration of certain BA species activates intestine FXR, which contributes to the beneficial effects of SNN on NASH. Although we revealed the relationship of SNN treatment, gut microbiota, BA profile and NASH, the exact mechanisms still need to be elucidated, especially the role of specific gut microbiome and BA species in the regulation of biological processes. Here we applied a typical NASH animal model, and the findings need to be verified in other animal models and also in clinic.

Funding

This work was supported by grants from the National Natural Science Foundation of China (No. 81774084, 81803897 and 81804020). The funders had no role in study design, data collection and analysis, decision to publish, or preparation of the manuscript.

Author contributions

GJ and LZ designed the project. CL, WZ, ML and XS carried out experiments, collected the samples. CL, WZ and LZ interpreted the data, drafted and edited the manuscript, GJ supervised the process and revised the manuscript. All authors have read and approved the final manuscript.

Conflict of interest statement

The authors declare that the research was conducted in the absence of any commercial or financial relationships that could be construed as a potential conflict of interest.

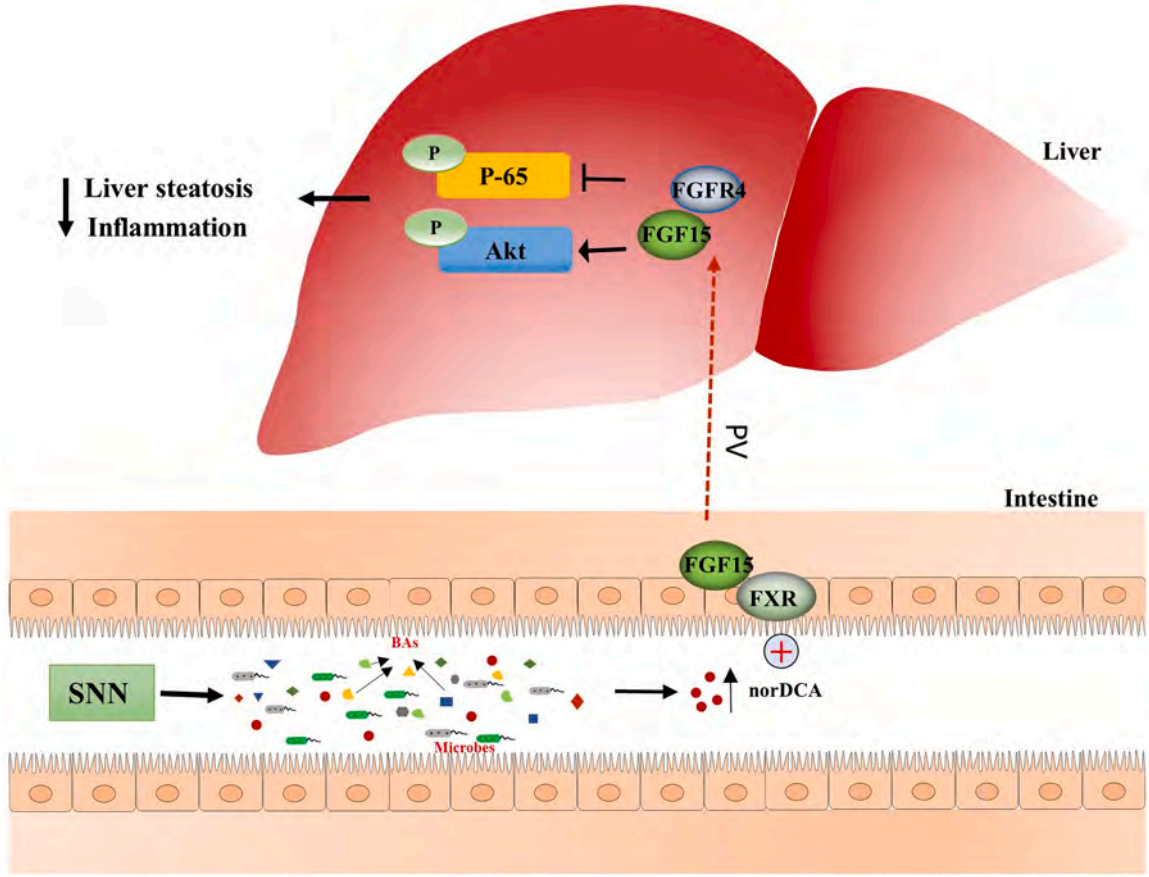

Fig. 7. Potential mechanisms of SNN on NASH. SNN treatment modulates gut microbiomes and related BA components, the altered BAs (eg. norDCA) further activate intestinal FXR-FGF15 pathway, thus enhance hepatic insulin sensitivity and suppress inflammatory status.

Acknowledgments

Not applicable.

References

[1] Z.M. Younossi, A.B. Koenig, D. Abdelatif, Y. Fazel, L. Henry, M. Wymer, Global epidemiology of nonalcoholic fatty liver disease-meta-analytic assessment of prevalence, incidence, and outcomes, Hepatology 64 (2016) 73–84, https://doi.org/10.1002/hep.28431.

[2] D. Goldberg, I.C. Ditah, K. Saeian, M. Lalehzari, A. Aronsohn, E.C. Gorospe, M. Charlton, Changes in the prevalence of hepatitis C virus infection, nonalcoholic steatohepatitis, and alcoholic liver disease among patients with cirrhosis or liver failure on the waitlist for liver transplantation, Gastroenterology 152 (2017) 1090–1099.e1091, https://doi.org/10.1053/j.gastro.2017.01.003.

[3] D.E. Kleiner, E.M. Brunt, M. Van Natta, C. Behling, M.J. Contos, O.W. Cummings, L. D. Ferrell, Y.C. Liu, M.S. Torbenson, A. Unalp-Arida, M. Yeh, A.J. McCullough, A. J. Sanyal, Design and validation of a histological scoring system for nonalcoholic fatty liver disease, Hepatology 41 (2005) 1313–1321, https://doi.org/10.1002/hep.20701.

[4] M.J. Armstrong, L.A. Adams, A. Canbay, W.K. Syn, Extrahepatic complications of nonalcoholic fatty liver disease, Hepatology 59 (2014) 1174–1197, https://doi.org/10.1002/hep.26717.

[5] G. den Besten, A. Bleeker, A. Gerding, K. van Eunen, R. Havinga, T.H. van Dijk, M. H. Oosterveer, J.W. Jonker, A.K. Groen, D.J. Reijngoud, B.M. Bakker, Short-chain fatty acids protect against high-fat diet-induced obesity via a PPARγ-dependent switch from lipogenesis to fat oxidation, Diabetes 64 (2015) 2398–2408, https://doi.org/10.2337/db14-1213.

[6] B. Sun, Y. Jia, J. Hong, Q. Sun, S. Gao, Y. Hu, N. Zhao, R. Zhao, Sodium butyrate ameliorates high-fat-diet-induced non-alcoholic fatty liver disease through peroxisome proliferator-activated receptor α-mediated activation of β oxidation and suppression of inflammation, J. Agric. Food Chem. 66 (2018) 7633–7642, https://doi.org/10.1021/acs.jafc.8b01189.

[7] T. Honda, M. Ishigami, F. Luo, M. Lingyun, Y. Ishizu, T. Kuzuya, K. Hayashi, I. Nakano, T. Ishikawa, G.G. Feng, Y. Katano, T. Kohama, Y. Kitaura, Y. Shimomura, H. Goto, Y. Hirooka, Branched-chain amino acids alleviate hepatic steatosis and liver injury in choline-deficient high-fat diet induced NASH mice, Metabol. Clin. Exp. 69 (2017) 177–187, https://doi.org/10.1016/j.metabol.2016.12.013.

[8] K. Takegoshi, M. Honda, H. Okada, R. Takabatake, N. Matsuzawa-Nagata, J. S. Campbell, M. Nishikawa, T. Shimakami, T. Shirasaki, Y. Sakai, T. Yamashita, T. Takamura, T. Tanaka, S. Kaneko, Branched-chain amino acids prevent hepatic fibrosis and development of hepatocellular carcinoma in a non-alcoholic steatohepatitis mouse model, Oncotarget 8 (2017) 18191–18205, https://doi.org/10.18632/oncotarget.15304.

[9] P. Puri, K. Daita, A. Joyce, F. Mirshahi, P.K. Santhekadur, S. Cazanave, V. A. Luketic, M.S. Siddiqui, S. Boyett, H.K. Min, D.P. Kumar, R. Kohli, H. Zhou, P. B. Hylemon, M.J. Contos, M. Idowu, A.J. Sanyal, The presence and severity of nonalcoholic steatohepatitis is associated with specific changes in circulating bile acids, Hepatology 67 (2018) 534–548, https://doi.org/10.1002/hep.29359.

[10] M.D. Chow, Y.H. Lee, G.L. Guo, The role of bile acids in nonalcoholic fatty liver disease and nonalcoholic steatohepatitis, Mol. Asp. Med. 56 (2017) 34–44, https://doi.org/10.1016/j.mam.2017.04.004.

[11] P.D. Petrov, M.V. García-Mediavilla, C. Guzmán, D. Porras, E. Nistal, S. Martínez-Flórez, J.V. Castell, J. González-Gallego, S. Sánchez-Campos, R. Jover, A network involving gut microbiota, circulating bile acids, and hepatic metabolism genes that protects against non-alcoholic fatty liver disease, Mol. Nutr. Food Res. 63 (2019), 1900487, https://doi.org/10.1002/mnfr.201900487.

[12] A. Wahlström, S.I. Sayin, H.U. Marschall, F. Bäckhed, Intestinal crosstalk between bile acids and microbiota and its impact on host metabolism, Cell Metab. 24 (2016) 41–50, https://doi.org/10.1016/j.cmet.2016.05.005.

[13] F. Huang, X. Zheng, X. Ma, R. Jiang, W. Zhou, S. Zhou, Y. Zhang, S. Lei, S. Wang, J. Kuang, X. Han, M. Wei, Y. You, M. Li, Y. Li, D. Liang, J. Liu, T. Chen, C. Yan, R. Wei, C. Rajani, C. Shen, G. Xie, Z. Bian, H. Li, A. Zhao, W. Jia, Theabrownin from Pu-erh tea attenuates hypercholesterolemia via modulation of gut microbiota and bile acid metabolism, Nat. Commun. 10 (2019) 4971, https://doi.org/10.1038/s41467-019-12896-x.

[14] Y. Liu, H. Song, L. Wang, H. Xu, X. Shu, L. Zhang, Y. Li, D. Li, G. Ji, Hepatoprotective and antioxidant activities of extracts from Salvia-Nelumbinis naturalis against nonalcoholic steatohepatitis induced by methionine- and choline-deficient diet in mice, J. Transl. Med 12 (2014) 315, https://doi.org/10.1186/s12967-014-0315-x.

[15] L. Zhang, J. Xu, H. Song, Z. Yao, G. Ji, Extracts from Salvia-Nelumbinis naturalis alleviate hepatosteatosis via improving hepatic insulin sensitivity, J. Transl. Med 12 (2014) 236, https://doi.org/10.1186/s12967-014-0236-8.

[16] X. Shu, M. Wang, H. Xu, Y. Liu, J. Huang, Z. Yao, L. Zhang, Extracts of Salvia-Nelumbinis naturalis ameliorate nonalcoholic steatohepatitis via inhibiting gut-derived endotoxin mediated TLR4/NF-κB activation, Evid. Based Complement. Altern. Med. 2017 (2017) 1–13, https://doi.org/10.1155/2017/9208314.
[17] S.I. Sayin, A. Wahlström, J. Felin, S. Jäntti, H.U. Marschall, K. Bamberg, B. Angelin, T. Hyötyläinen, M. Orešič, F. Bäckhed, Gut microbiota regulates bile acid metabolism by reducing the levels of tauro-beta-muricholic acid, a naturally occurring FXR antagonist, Cell Metab. 17 (2013) 225–235, https://doi.org/10.1016/j.cmet.2013.01.003.
[18] Z. Ma, X. Shu, J. Huang, H. Zhang, Z. Xiao, L. Zhang, Salvia-Nelumbinis naturalis formula improved inflammation in LPS stressed macrophages via upregulating microRNA-152, Mediat. Inflamm. 2017 (2017) 1–9, https://doi.org/10.1155/2017/5842747.
[19] Y.-L. Lu, M. Wang, L. Zhang, Y.-Q. He, L. Yang, C.-H. Wang, Z.-T. Wang, G. Ji, Simultaneous determination of six components in the 'Jiang-Zhi' granule by UPLC-MS analysis, Chin. J. Nat. Med. 8 (2010) 449–455.
[20] T. Wu, J.M. Chen, T.G. Xiao, X.B. Shu, H.C. Xu, L.L. Yang, L.J. Xing, P.Y. Zheng, G. Ji, Qinggan Huoxue recipe suppresses epithelial-to-mesenchymal transition in alcoholic liver fibrosis through TGF-β1/Smad signaling pathway, World J. Gastroenterol. 22 (2016) 4695–4706, https://doi.org/10.3748/wjg.v22.i19.4695.
[21] Q. Li, M. Li, F. Li, W. Zhou, Y. Dang, L. Zhang, G. Ji, Qiang-Gan formula extract improves non-alcoholic steatohepatitis via regulating bile acid metabolism and gut microbiota in mice, J. Ethnopharmacol. 258 (2020), 112896, https://doi.org/10.1016/j.jep.2020.112896.
[22] A. Schmid, H. Neumann, T. Karrasch, G. Liebisch, A. Schäffler, Bile acid metabolome after an oral lipid tolerance test by liquid chromatography-tandem mass spectrometry (LC-MS/MS), PLoS One 11 (2016), e0148869, https://doi.org/10.1371/journal.pone.0148869.
[23] X. Zheng, F. Huang, A. Zhao, S. Lei, Y. Zhang, G. Xie, T. Chen, C. Qu, C. Rajani, B. Dong, D. Li, W. Jia, Bile acid is a significant host factor shaping the gut microbiome of diet-induced obese mice, BMC Biol. 15 (2017) 120, https://doi.org/10.1186/s12915-017-0462-7.
[24] M. Mouzaki, E.M. Comelli, B.M. Arendt, J. Bonengel, S.K. Fung, S.E. Fischer, I. D. McGilvray, J.P. Allard, Intestinal microbiota in patients with nonalcoholic fatty liver disease, Hepatology 58 (2013) 120–127, https://doi.org/10.1002/hep.26319.
[25] A. Koliada, G. Syzenko, V. Moseiko, L. Budovska, K. Puchkov, V. Perederiy, Y. Gavalko, A. Dorofeyev, M. Romanenko, S. Tkach, L. Sineok, O. Lushchak, A. Vaiserman, Association between body mass index and Firmicutes/Bacteroidetes ratio in an adult Ukrainian population, BMC Microbiol. 17 (2017) 120, https://doi.org/10.1186/s12866-017-1027-1.
[26] R.P. Durk, E. Castillo, L. Márquez-Magaña, G.J. Grosicki, N.D. Bolter, C.M. Lee, J. R. Bagley, Gut microbiota composition is related to cardiorespiratory fitness in healthy young adults, Int J. Sport Nutr. Exerc. Metab. 29 (2019) 249–253, https://doi.org/10.1123/ijsnem.2018-0024.
[27] F.Z. Marques, E. Nelson, P.Y. Chu, D. Horlock, A. Fiedler, M. Ziemann, J.K. Tan, S. Kuruppu, N.W. Rajapakse, A. El-Osta, C.R. Mackay, D.M. Kaye, High-fiber diet and acetate supplementation change the gut microbiota and prevent the development of hypertension and heart failure in hypertensive mice, Circulation 135 (2017) 964–977, https://doi.org/10.1161/circulationaha.116.024545.
[28] C. Kong, R. Gao, X. Yan, L. Huang, H. Qin, Probiotics improve gut microbiota dysbiosis in obese mice fed a high-fat or high-sucrose diet, Nutrition 60 (2019) 175–184, https://doi.org/10.1016/j.nut.2018.10.002.
[29] J.C. Whittemore, J.E. Stokes, J.M. Price, J.S. Suchodolski, Effects of a synbiotic on the fecal microbiome and metabolomic profiles of healthy research cats administered clindamycin: a randomized, controlled trial, Gut Microbes 10 (2019) 521–539, https://doi.org/10.1080/19490976.2018.1560754.
[30] C.J. Martoni, A. Labbé, J.G. Ganopolsky, S. Prakash, M.L. Jones, Changes in bile acids, FGF-19 and sterol absorption in response to bile salt hydrolase active L. reuteri NCIMB 30242, Gut Microbes 6 (2015) 57–65, https://doi.org/10.1080/19490976.2015.1005474.
[31] P.M. Ryan, E.H. Stolte, L.E.E. London, J.M. Wells, S.L. Long, S.A. Joyce, C.G. M. Gahan, G.F. Fitzgerald, R.P. Ross, N.M. Caplice, C. Stanton, Lactobacillus mucosae DPC 6426 as a bile-modifying and immunomodulatory microbe, BMC Microbiol. 19 (2019) 33, https://doi.org/10.1186/s12866-019-1403-0.
[32] M. Vital, T. Rud, S. Rath, D.H. Pieper, D. Schlüter, Diversity of bacteria exhibiting bile acid-inducible 7α-dehydroxylation genes in the human gut, Comput. Struct. Biotechnol. J. 17 (2019) 1016–1019, https://doi.org/10.1016/j.csbj.2019.07.012.
[33] T. Chouvenc, M.L. Elliott, J. Šobotník, C.A. Efstathion, N.Y. Su, The termite fecal nest: a framework for the opportunistic acquisition of beneficial soil streptomyces (Actinomycetales: Streptomycetaceae), Environ. Entomol. 47 (2018) 1431–1439, https://doi.org/10.1093/ee/nvy152.
[34] K. Huang, Y. Yan, D. Chen, Y. Zhao, W. Dong, X. Zeng, Y. Cao, Ascorbic acid derivative 2-O-β-d-glucopyranosyl-l-ascorbic acid from the fruit of lycium barbarum modulates microbiota in the small intestine and colon and exerts an immunomodulatory effect on cyclophosphamide-treated BALB/c mice, J. Agric. Food Chem. 68 (2020) 11128–11143, https://doi.org/10.1021/acs.jafc.0c04253.
[35] Y. Tang, J. Zhang, J. Li, X. Lei, D. Xu, Y. Wang, C. Li, X. Li, Y. Mao, Turnover of bile acids in liver, serum and caecal content by high-fat diet feeding affects hepatic steatosis in rats, Biochim. Biophys. Acta Mol. Cell Biol. Lipids 1864 (2019) 1293–1304, https://doi.org/10.1016/j.bbalip.2019.05.016.
[36] P. Fickert, G.M. Hirschfield, G. Denk, H.U. Marschall, I. Altorjay, M. Färkkilä, C. Schramm, U. Spengler, R. Chapman, A. Bergquist, E. Schrumpf, F. Nevens, P. Trivedi, F.P. Reiter, I. Tornai, E. Halilbasic, R. Greinwald, M. Pröls, M.P. Manns, M. Trauner, norUrsodeoxycholic acid improves cholestasis in primary sclerosing cholangitis, J. Hepatol. 67 (2017) 549–558, https://doi.org/10.1016/j.jhep.2017.05.009.
[37] D. Steinacher, T. Claudel, M. Trauner, Therapeutic mechanisms of bile acids and nor-ursodeoxycholic acid in non-alcoholic fatty liver disease, Dig. Dis. 35 (2017) 282–287, https://doi.org/10.1159/000454853.
[38] H. Wu, G. Liu, Y. He, J. Da, B. Xie, Obeticholic acid protects against diabetic cardiomyopathy by activation of FXR/Nrf2 signaling in db/db mice, Eur. J. Pharmacol. 858 (2019), 172393, https://doi.org/10.1016/j.ejphar.2019.05.022.
[39] C. Jiang, C. Xie, Y. Lv, J. Li, K.W. Krausz, J. Shi, C.N. Brocker, D. Desai, S.G. Amin, W.H. Bisson, Y. Liu, O. Gavrilova, A.D. Patterson, F.J. Gonzalez, Intestine-selective farnesoid X receptor inhibition improves obesity-related metabolic dysfunction, Nat. Commun. 6 (2015) 10166, https://doi.org/10.1038/ncomms10166.
[40] F.J. Gonzalez, C. Jiang, C. Xie, A.D. Patterson, Intestinal farnesoid X receptor signaling modulates metabolic disease, Dig. Dis. 35 (2017) 178–184, https://doi.org/10.1159/000450908.
[41] B. Kong, M. Zhang, M. Huang, D. Rizzolo, L.E. Armstrong, J.D. Schumacher, M. D. Chow, Y.H. Lee, G.L. Guo, FXR deficiency alters bile acid pool composition and exacerbates chronic alcohol induced liver injury, Dig. Liver Dis. 51 (2019) 570–576, https://doi.org/10.1016/j.dld.2018.12.026.
[42] P. Hartmann, K. Hochrath, A. Horvath, P. Chen, C.T. Seebauer, C. Llorente, L. Wang, Y. Alnouti, D.E. Fouts, P. Stärkel, R. Loomba, S. Coulter, C. Liddle, R. T. Yu, L. Ling, S.J. Rossi, A.M. DePaoli, M. Downes, R.M. Evans, D.A. Brenner, B. Schnabl, Modulation of the intestinal bile acid/farnesoid X receptor/fibroblast growth factor 15 axis improves alcoholic liver disease in mice, Hepatology 67 (2018) 2150–2166, https://doi.org/10.1002/hep.29676.
[43] M. Song, J. Ye, F. Zhang, H. Su, X. Yang, H. He, F. Liu, X. Zhu, L. Wang, P. Gao, G. Shu, Q. Jiang, S. Wang, Chenodeoxycholic acid (CDCA) protects against the lipopolysaccharide-induced impairment of the intestinal epithelial barrier function via the FXR-MLCK pathway, J. Agric. Food Chem. 67 (2019) 8868–8874, https://doi.org/10.1021/acs.jafc.9b03173.
[44] M. Sorribas, M.O. Jakob, B. Yilmaz, H. Li, D. Stutz, Y. Noser, A. de Gottardi, S. Moghadamrad, M. Hassan, A. Albillos, R. Francés, O. Juanola, I. Spadoni, M. Rescigno, R. Wiest, FXR modulates the gut-vascular barrier by regulating the entry sites for bacterial translocation in experimental cirrhosis, J. Hepatol. 71 (2019) 1126–1140, https://doi.org/10.1016/j.jhep.2019.06.017.
[45] R. Sun, N. Yang, B. Kong, B. Cao, D. Feng, X. Yu, C. Ge, J. Huang, J. Shen, P. Wang, S. Feng, F. Fei, J. Guo, J. He, N. Aa, Q. Chen, Y. Pan, J.D. Schumacher, C.S. Yang, G. L. Guo, J. Aa, G. Wang, Orally administered berberine modulates hepatic lipid metabolism by altering microbial bile acid metabolism and the intestinal FXR signaling pathway, Mol. Pharm. 91 (2017) 110–122, https://doi.org/10.1124/mol.116.106617.